Progress In Electromagnetics Research, Vol. 118, 487–504, 2011

STUDY OF NONRECIPROCAL DEVICES USING THREE-STRIP FERRITE COUPLED LINE

W. Marynowski* **and J. Mazur**

Faculty of Electronics, Telecommunications and Informatics, Gdansk University of Technology, Gdansk, Poland

Abstract—This paper presents the investigations of nonreciprocal devices employing a novel ferrite coupled line junction. The structure is designed using coplanar line technology with the ground half-planes reduced to the strips. The investigated junction is composed of one ferrite section placed in between of two dielectric sections. In the ferrite section the longitudinally magnetized ferrite slab is located at the top or the bottom of the strips and is covered with the dielectric layers. In the dielectric sections the ports of the junctions are located. The wave parameters and field distributions of the modes propagated in the dielectric and ferrite sections are obtained from spectral domain approach. In order to determine the scattering matrix of the junction the mode matching method is utilized. The investigation of the circulator and isolator designed based on the S-matrix of the junction are presented. The obtained results are verified by comparing them with HFSS simulations and own measurements of the fabricated devices. In both cases a very good agreement is observed.

1. INTRODUCTION

Nonreciprocal devices are important components of the modern microwave systems [1–19]. In order to obtain the nonreciprocal effects one needs to utilize the ferrite materials [1–18] or active elements such as amplifiers [19]. The integrated nonreciprocal devices are in general realized in microstrip [2–12] or slot line [15–18] technology, with the ferrite material magnetized longitudinally or transversely. Recently, the longitudinally magnetized microstrip [2–11] or slot [17, 18] ferrite

Received 17 May 2011, Accepted 24 June 2011, Scheduled 13 July 2011
* Corresponding author: Wojciech Marynowski (wojmar@eti.pg.gda.pl).

coupled lines (FCL) are being developed and employed to realize integrated nonreciprocal devices. Generally, the FCL section is a four port circuit build with a standard coupled lines (CL) composed of three conductors and with ferrite slab located above or below the lines. In the standard CL section, without the ferrite, two dominant modes (even and odd) are propagated with no cut-off frequency. The nonreciprocity of the FCL, introduced by a ferrite slab, results from gyromagnetic coupling of these two waves as was shown in [1, 2] with the use of coupled mode method (CMM). This coupling occurs when the location of the ferrite slab coincides with the location of the transverse magnetic field vectors of these two waves being orthogonal [1]. This phenomenon leads to the excitation of two waves propagating with different phase coefficients in the FCL section. Unlike the standard CL the waves in FCL section have the cut-off frequency. It appears in this structure near the frequency for which the effective permeability of the ferrite slab is equal zero ($\mu_{eff}(f_{\text{cut-off}}) = 0$). The differential phase shift between these waves defines the angle of Faraday rotation phenomenon which appears in the ferrite guide as a result of gyromagnetic coupling. When utilizing the FCL sections to the construction of circulators, their advantages, in comparison to conventional circulators, are wide bandwidth and weak bias magnetic field required for their nonreciprocal operation. Moreover, the special requirements for the fabrication of the ferrite sample are not needed even for the millimeter-wave bands. However, in such structures high insertion losses associated with long ferrite slab (often several wavelengths) are being observed. Recent researches on these devices concern improvement of their parameters such as bandwidth and losses [3–10, 17]. Taking into consideration the Faraday effect that appears in the structure, the optimal behavior of FCL section is obtained for ferrite interaction with linearly or circularly polarized waves [3, 12].

In this paper we consider the previously proposed section of multilayer FCL [20, 21] shown in Fig. 1(a). The investigated junction using proposed FCL section terminated with dielectric sections is presented in Fig. 1(b). The proposed structure is similar to the conventional coplanar line, though the infinite ground half-planes are reduced to the strips. In comparison to previously analyzed structure [11] two additional dielectric layers are introduced: dielectric 1 and dielectric 2 in Fig. 1(a).

In our previous work [20, 21] the considered junction was investigated with the use of coupled-mode method (CMM). In this paper the wave parameters and fields distributions of two fundamental modes propagated in the ferrite and dielectric sections are determined

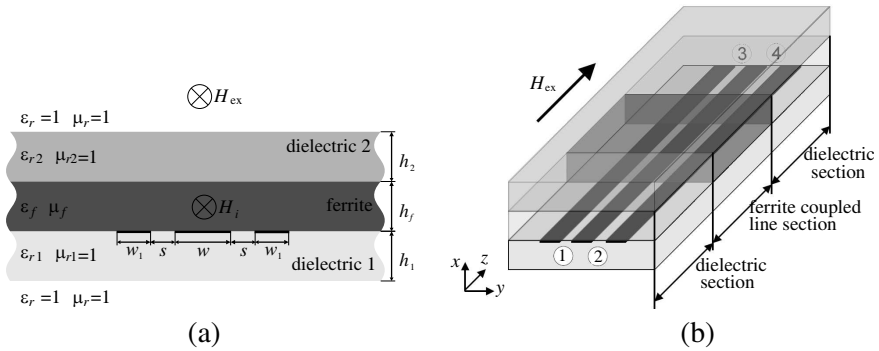

Figure 1. Analyzed structure: (a) cross section, (b) general view; H_i — internal magnetic field, H_{ex} — external magnetic field.

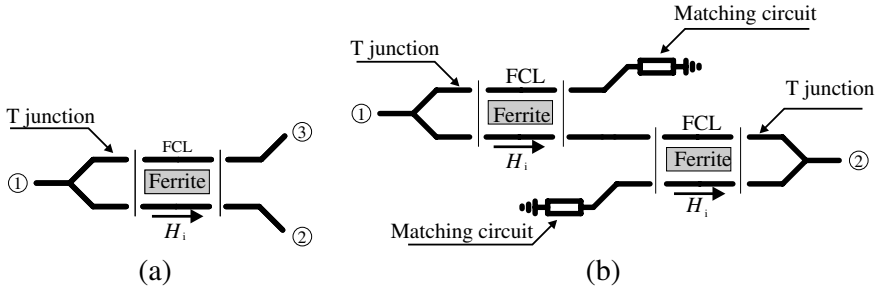

Figure 2. Schematic configurations of analyzed structures: (a) FCL circulator, (b) FCL double isolator.

using spectral domain approach (SDA). Using obtained results the scattering matrix of three-strip FCL junction is calculated utilizing software, based on mode matching (MM) method [12]. The obtained S-matrix is used to design nonreciprocal devices. The first application of the proposed three-strip FCL junction is a circulator, which is schematically presented in Fig. 2(a). The circulator is composed of the FCL junction cascaded with a T-junction. The next designed device is a double isolator, which is schematically presented in Fig. 2(b). This circuit is composed of two FCL circulators with two ports terminated with matched loads. The above presented structures are designed, fabricated and measured. The obtained numerical results are compared with experimental ones and discussed.

2. SCATTERING MATRIX MODEL OF THE FCL JUNCTION

In order to determine the S-matrix of the proposed FCL junction the mode matching method is utilized. At first the junction is analyzed as a two port structure composed of dielectric section followed by ferrite section and another dielectric section as presented in Fig. 3. Since the widths of the strips in the ferrite and dielectric sections are the same the higher modes are not excited, hence, they are not considered in the analysis. In each section only two fundamental modes are taken into consideration. The modes propagated in the dielectric and ferrite sections are called dielectric and ferrite waves, respectively. Due to the symmetry of the structure we can distinguished even- and odd-mode waves in the dielectric section. Despite the fact, that at port ① or ② only one of the dielectric waves can appear, both ferrite waves are excited.

The wave parameters and field distributions of modes in the ferrite and dielectric sections are determined using SDA [11]. The total field in each section is determined as a superposition of both modes propagating in forward (+) and backward (−) directions. Using notation from Fig. 3 the total field in dielectric sections can be written in the following form:

$$\mathbf{F}_t^{(i)} = \left[\mathbf{F}_{+e}^{(i)}, \quad \mathbf{F}_{+o}^{(i)}, \quad \mathbf{F}_{-e}^{(i)}, \quad \mathbf{F}_{-o}^{(i)}\right] \begin{bmatrix} A_e^{(i)} \\ A_o^{(i)} \\ B_e^{(i)} \\ B_o^{(i)} \end{bmatrix}, \tag{1}$$

where $\mathbf{F} = (\mathbf{E}, \mathbf{H})$ represents tangential electric or magnetic field, A and B are the unknown expansion coefficients describing forward and backward waves, respectively, of even (e) and odd (o) modes, superscript $i = (1, 2)$ determines the number of dielectric section. The total field in ferrite section can be written as follows:

$$\mathbf{F}_t^{(0)} = \left[\mathbf{F}_{+1}^{(0)}, \quad \mathbf{F}_{+2}^{(0)}, \quad \mathbf{F}_{-1}^{(0)}, \quad \mathbf{F}_{-2}^{(0)}\right] \mathbf{D}(z) \begin{bmatrix} C_{+1}^{(0)} \\ C_{+2}^{(0)} \\ C_{-1}^{(0)} \\ C_{-2}^{(0)} \end{bmatrix}, \tag{2}$$

where $\mathbf{D}(z) = \mathrm{diag}([e^{\mathrm{j}\beta_{+1}^{(0)}z}, e^{\mathrm{j}\beta_{+2}^{(0)}z}, e^{\mathrm{j}\beta_{-1}^{(0)}z}, e^{\mathrm{j}\beta_{-2}^{(0)}z}])$, $\beta_{\pm 1(2)}^{(0)}$ are the propagation coefficients of both fundamental modes in ferrite section, $\mathbf{F} = (\mathbf{E}, \mathbf{H})$ represents tangential electric or magnetic field and C

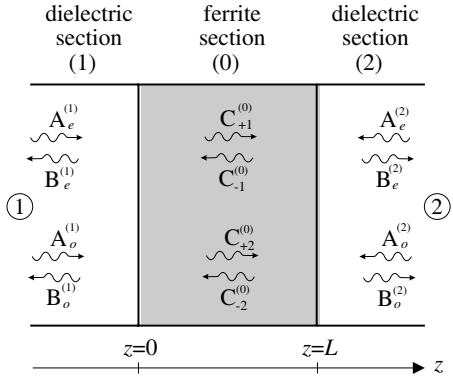

Figure 3. Two port FCL junction composed of ferrite and dielectric sections.

are the unknown expansion coefficients describing forward (+) and backward (−) waves. Using relations (1) and (2) the continuity conditions for the tangential components of electric and magnetic fields at two interfaces $z = 0$ and $z = L$ can be written as follows:

$$\mathbf{E}_t^{(1)}\big|_{z=0} = \mathbf{E}_t^{(0)}\big|_{z=0}, \quad \mathbf{H}_t^{(1)}\big|_{z=0} = \mathbf{H}_t^{(0)}\big|_{z=0}, \tag{3}$$

$$\mathbf{E}_t^{(2)}\big|_{z=L} = \mathbf{E}_t^{(0)}\big|_{z=L}, \quad \mathbf{H}_t^{(2)}\big|_{z=L} = \mathbf{H}_t^{(0)}\big|_{z=L}. \tag{4}$$

This set of equations can be solved using the orthogonality expansion method. As a result the set of linear equations is obtained, which can be written in the matrix form as follows:

$$\begin{bmatrix} \mathbf{X}_1 & \mathbf{X}_2 & \mathbf{X}_3 \\ \mathbf{X}_4 & \mathbf{X}_5 & \mathbf{X}_6 \end{bmatrix} \begin{bmatrix} \mathbf{A}' \\ \mathbf{B}' \\ \mathbf{C}' \end{bmatrix} = 0, \tag{5}$$

where $\mathbf{A}'$, $\mathbf{B}'$ and $\mathbf{C}'$ are the vectors of unknown expansion coefficients for the fields in each section $\mathbf{A}' = [A_e^{(1)}, A_o^{(1)}, A_e^{(2)}, A_o^{(2)}]^T$, $\mathbf{B}' = [B_e^{(1)}, B_o^{(1)}, B_e^{(2)}, B_o^{(2)}]^T$, $\mathbf{C}' = [C_{+1}^{(0)}, C_{+2}^{(0)}, C_{-1}^{(0)}, C_{-2}^{(0)}]^T$ and the matrices $\mathbf{X}$ are defined in Appendix A.

The relations between $\mathbf{A}'$ and $\mathbf{B}'$ can be written as follows:

$$\mathbf{B}' = \mathbf{S}'\mathbf{A}', \tag{6}$$

where

$$\mathbf{S}' = \begin{bmatrix} S_{ee}^{11} & S_{eo}^{11} & S_{ee}^{12} & S_{eo}^{12} \\ S_{oe}^{11} & S_{oo}^{11} & S_{oe}^{12} & S_{oo}^{12} \\ S_{ee}^{21} & S_{eo}^{21} & S_{ee}^{22} & S_{eo}^{22} \\ S_{oe}^{21} & S_{oo}^{21} & S_{oe}^{22} & S_{oo}^{22} \end{bmatrix}. \tag{7}$$

The $\mathbf{S}'$ matrix defines two mode scattering matrix of two port FCL junction. The element S_{nm}^{ji} defines the relation between m incident wave in the ith port and n reflected wave in the jth port, where $m, n = \{e, o\}$ and $i, j = \{1, 2\}$. Using relation (5) matrix $\mathbf{S}'$ can be defined as follows

$$\mathbf{S}' = -\left(\mathbf{X}_5 - \mathbf{X}_6\mathbf{X}_3^{-1}\mathbf{X}_2\right)^{-1}\left(\mathbf{X}_4 - \mathbf{X}_6\mathbf{X}_3^{-1}\mathbf{X}_1\right). \tag{8}$$

In the designing procedure of the integrated nonreciprocal devices more useful is the S-matrix defined from the point of view of the incident and reflected waves at four ports of FCL junction. The scheme of such junction is presented in Fig. 4. Using the symmetry properties of the even and odd modes propagated in the dielectric sections the matrix $\mathbf{S}'$ can be rearranged in terms of port waves and finally the scattering matrix of four port FCL junction is obtained. The incident and reflected waves at ith port are denoted by $A^{(i)}$ and $B^{(i)}$, respectively. Due to symmetry of the waves in the dielectric sections they can be written as a superpositions of waves in each port of four port FCL junction as follows:

$$\begin{aligned} A_e^{(1)} &= A^{(1)} + A^{(2)}, \quad A_o^{(1)} = A^{(1)} - A^{(2)}, \\ B_e^{(1)} &= B^{(1)} + B^{(2)}, \quad B_o^{(1)} = B^{(1)} - B^{(2)}, \\ A_e^{(2)} &= A^{(3)} + A^{(4)}, \quad A_o^{(2)} = A^{(3)} - A^{(4)}, \\ B_e^{(2)} &= B^{(3)} + B^{(4)}, \quad B_o^{(2)} = B^{(3)} - B^{(4)}. \end{aligned} \tag{9}$$

which can be expressed in the matrix form:

$$\mathbf{A}' = \mathbf{T}\mathbf{A} \quad \text{and} \quad \mathbf{B}' = \mathbf{T}\mathbf{B}, \tag{10}$$

where $\mathbf{A} = [A^{(1)}, A^{(2)}, A^{(3)}, A^{(4)}]^T$, $\mathbf{B} = [B^{(1)}, B^{(2)}, B^{(3)}, B^{(4)}]^T$ and

$$\mathbf{T} = \begin{bmatrix} \mathbf{T}_1 & 0 \\ 0 & \mathbf{T}_1 \end{bmatrix}, \quad \mathbf{T}_1 = \begin{bmatrix} 1 & 1 \\ 1 & -1 \end{bmatrix}. \tag{11}$$

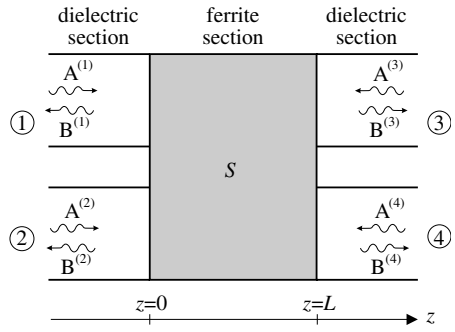

Figure 4. Four port FCL junction.

Finally, using the two mode S-matrix (6)and relations (10), the scattering matrix of the four port FCL junction is obtained

$$\mathbf{B} = \mathbf{SA}, \quad \text{where} \quad \mathbf{S} = \mathbf{T}^{-1}\,\mathbf{S}'\,\mathbf{T}. \tag{12}$$

Such S-matrix can be used in the analysis of the transmission properties of FCL junction with the assumed excitation.

3. FCL STRUCTURE — NUMERICAL RESULTS

The numerical investigations presented in this section consider the FCL structure presented in Fig. 1 with the following dimensions and parameters: $h_1 = h_2 = 0.508\,\text{mm}$, $h_f = 0.5\,\text{mm}$, $w_1 = w = 0.4\,\text{mm}$, $s = 0.3\,\text{mm}$, $\varepsilon_{r1} = 2.2$, $\varepsilon_{r2} = 9.6$, $\varepsilon_f = 13.3$, magnetization saturation of the ferrite material $4\pi Ms = 3000\,\text{Gauss}$, gyromagnetic ratio $\gamma = 2.8\,\text{MHz/Gauss}$, half value of resonance width $\Delta H = 0$ and internal magnetic field $H_i = 0$. The dispersion characteristics of the two fundamental modes in the ferrite and dielectric sections obtained from SDA [11] are presented in Fig. 5. It can be seen that two fundamental modes in the dielectric section are propagated without cut-off frequency, while cut-off frequency of the modes in the ferrite section is close to $f_c = \gamma(H_i + M_s)$. It means that the ferrite waves propagate when $\mu_{eff} = (\mu^2 - \mu_a^2)/\mu > 0$.

Next, the scattering parameters in a function of length of the ferrite L at center frequency $f_0 = 13\,\text{GHz}$ are calculated and depicted in

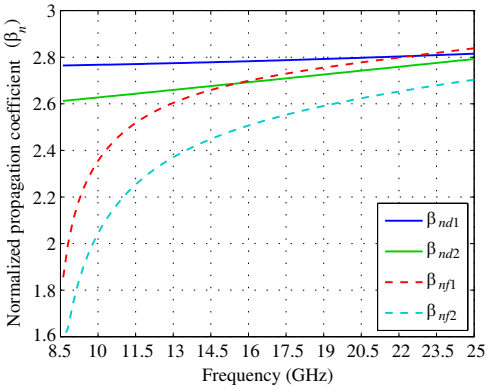

Figure 5. Normalized dispersion characteristics ($\beta_n = \beta/k_0$) of two fundamental modes in dielectric section (β_{nd1}, β_{nd2}) and ferrite section (β_{nf1}, β_{nf2}) for the structure from Fig. 1.

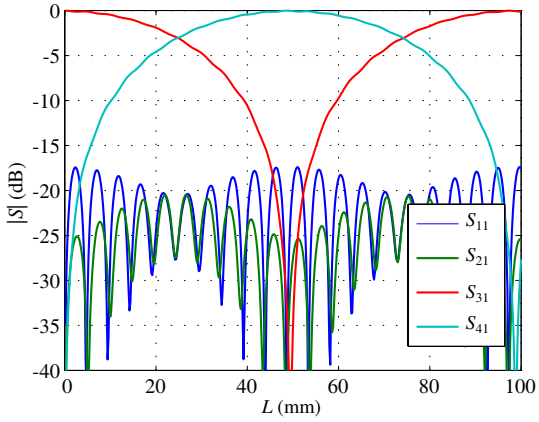

Figure 6. Predicted scattering matrix in a function of length of the ferrite at $f_0 = 13\,\text{GHz}$ for FCL junction from Fig. 1.

Fig. 6. Length $L_f = 24.8\,\text{mm}$ of the ferrite ensures equal output signals at ports ③ and ④ for the excitation in port ①. When the length of the ferrite is doubled ($L = 2L_f$) the output signal appears only in port ④, while port ③ is isolated. The periodic transfer of energy between slots of the FCL also can be observed in Fig. 7, where the change of the power density distribution along the structure is shown. For $z = 0$ the energy of the signal is concentrated around one of the FCL slots, but for $z = L_f$ signal is divided between two slots. For $z = 2L_f$ the energy of the signal is concentrated around the second slot of FCL. This effect is periodic and it repeats for length $L = 4L_f$. The obtained length $L_f = 24.8\,\text{mm}$ of the ferrite section is used to calculate the frequency response of the FCL junction. It can be seen from Fig. 8(a), that equal transmissions to ports ③ and ④ ($-3\,\text{dB}$ $\pm 0.5\,\text{dB}$) are achieved in the frequency range from 10.5 GHz to 16 GHz, where the reflection losses and isolation are better than 20 dB. The obtained results were verified via simulation of the investigated structure in commercial software HFSS (see Fig. 8(b)) and as can be seen a good agreement between the results was achieved. To simplify and speed-up our MM analysis of FCL junction only two dominant modes in dielectric and ferrite sections were used to solve the problem, under the assumption that the higher modes are evanescent. It provides some small discrepancies between the scattering characteristics obtained from our approach and HFSS, however the obtained accuracy is more than satisfactory.

In the simulations the lossless ferrite section was considered. The losses appearing in the FCL junction result from the dielectric and

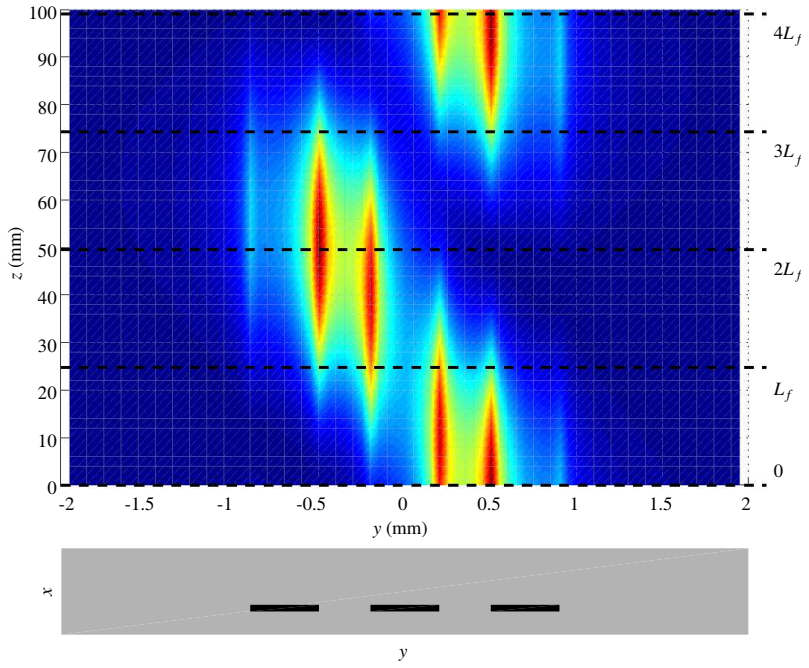

Figure 7. Power density distribution along the FCL junction from Fig. 1 at $f_0 = 13\,\text{GHz}$.

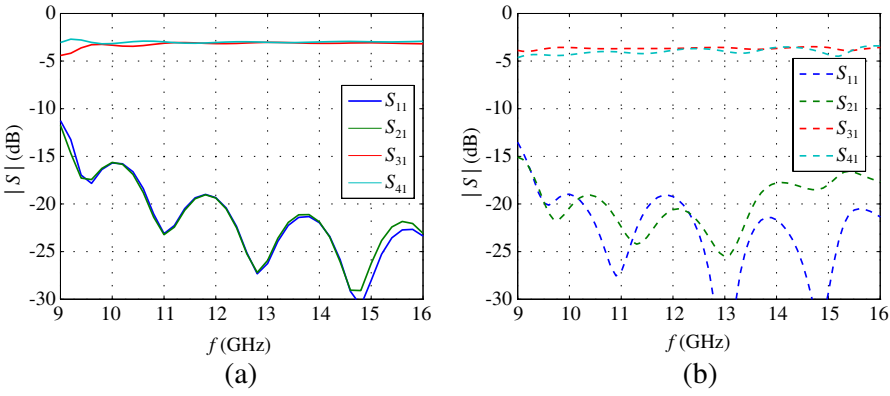

Figure 8. Scattering matrix versus frequency for the length of the ferrite $L_f = 24.8\,\text{mm}$. (a) Our method. (b) HFSS.

Table 1. Total losses of the considered FCL junction from Fig. 1 estimated at the frequency $f = 13\,\mathrm{GHz}$ (material parameters: $\tan\delta_1 = 0.003$, $\tan\delta_f = 0.0005$, $\tan\delta_2 = 0.0035$, $\Delta H = 190\,\mathrm{Oe}$ and $\sigma = 5.813 \cdot 10^7\,\mathrm{S/m}$).

losses (dB)			
conducting	dielectric	magnetic	total
0.08	0.17	0.98	1.23

ferrite material and the metallic strips. The dielectric and magnetic losses are defined by $\tan\delta$ and linewidth ΔH of the ferrite, respectively. The conductance σ of the metallic strips defines the conducting losses. The total losses of the considered FCL junction were estimated with the use of HFSS software and their values are presented in Table 1. It can be noticed that the total losses are equal to 1.23 dB and mainly result from the magnetic losses in the ferrite material equal to 0.98 dB.

In the proposed method it is sufficient to know the fields only in the cross-section of dielectric and ferrite sections in order to calculate the scattering parameters of the structure of arbitrary length. In any commercial software which is based on space-discretisation techniques the calculations requires to discretize the whole structure, resulting in a very slow performance of algorithms for large and complex configurations. For the investigated examples the proposed method allows one to obtain the results at least three times faster than by using HFSS. The speed of the method permits its use in an optimization process.

4. MULTILAYER THREE-STRIP FCL DEVICES

In this section the examples of applications of analyzed FCL junction are presented. In the analysis the structure characterized by S-matrix presented in Fig. 8 was utilized. The investigated structures of FCL circulator and double isolator were manufactured and measured. The ferrite samples in FCL section were longitudinally magnetized with suitable external magnetic bias H_{ex} (see Fig. 1) provided by proper set of magnets. Measurements were performed with the use of Wiltron 37267 VNA with the standard SOLT calibration.

4.1. Circulator

At first the FCL circulator was designed by cascading the FCL junction with the T-junction as it is shown in Fig. 2(a). The calculated

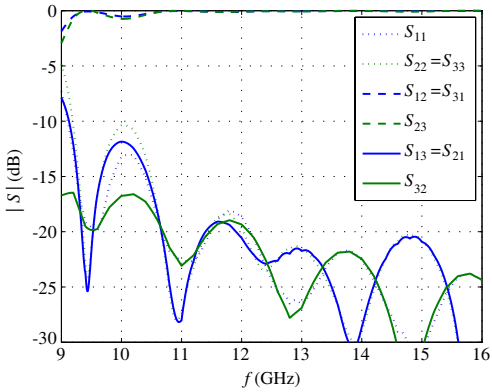

Figure 9. Predicted scattering matrix of the ferrite coupled line circulator.

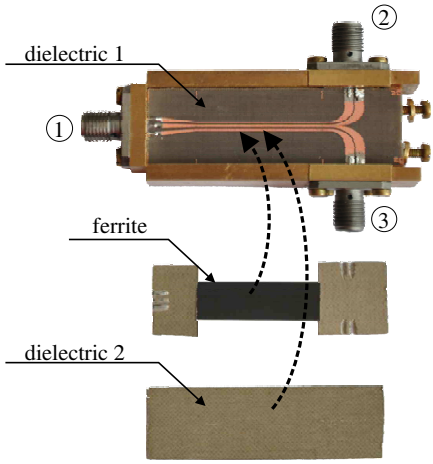

Figure 10. Photograph of the fabricated FCL circulator.

frequency response of the circulator containing ideal T-junction is shown in Fig. 9. It can be seen that the average isolations and reflection losses are about 20 dB near the designed operation frequency $f_0 = 13$ GHz. In the analysis the losses of FCL junction were neglected, hence the simulated transmissions of FCL circulator are about 0 dB. The structure of the circulator investigated theoretically was fabricated and measured. In the experiment, the middle strip was assumed to be a signal line, while the side strips were connected to the ground. The even excitation was realized directly from three-strip line. At

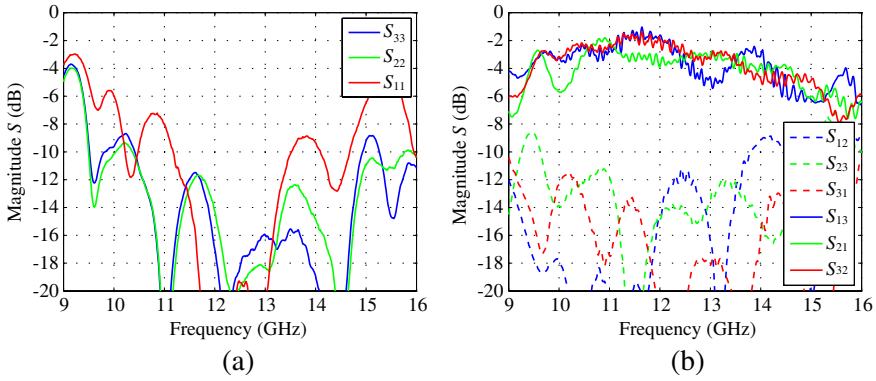

Figure 11. Measured scattering matrix of the FCL circulator: (a) reflection losses, (b) insertion losses and isolations.

the output of FCL, the coplanar three-strip structure was divided into two symmetric two-strip lines. In Fig. 10 a photograph of the fabricated FCL circulator is presented. The results of the circulator measurements are shown in Fig. 11. The average isolation is about 12 dB and insertion losses are about 2.7 dB in the frequency band 10–14 GHz. The values of the measured insertion losses are similar to the ones previously presented in FCL devices [3–7, 10, 17]. The total calculated using HFSS insertion losses of the FCL circulator comprise of the losses of FCL junction (about 1.23 dB — see Table 1) and T-junction and output lines (about 1 dB). It gives the value of total losses equal to 2.23 dB. It is worth noticing, that the obtained average measured values of the insertion losses equal 2.7 dB and is close to the predicted in the simulations.

In the frequency range 10–14 GHz the reflection losses at ports ② and ③ are better than 12 dB, whereas at port ① reflection losses are better than 12 dB in the frequency range from 11.3 GHz to 13.3 GHz. This is the effect of the parasitic capacitances produced during soldering of the connector.

4.2. Double Isolator

In the experimental investigations two structures of the double isolator were considered. The first structure was obtained cascading two FCL circulators with the remaining ports terminated using coaxial loads. The second one was an integrated planar structure where ports were matched with lumped resistors.

The measurement results of the first investigated structure of the

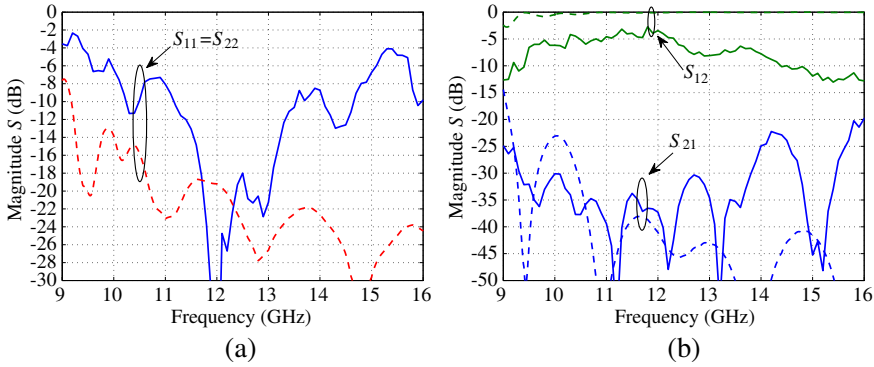

Figure 12. Scattering matrix of the double isolator obtained by using simulated (dashed line) and measured (solid line) characteristics of the FCL circulator: (a) reflection losses, (b) insertion losses and isolations.

double isolator are depicted in Fig. 12 (solid lines). The results are compared with the ones calculated by cascading simulated responses (from Fig. 9) of two circulators (dashed lines in Fig. 12). As it was previously mentioned, the insertion losses of FCL junction were not considered in the analysis. It can be seen from the results, by assuming the losses of one FCL section to be about 2–3 dB [3], the obtained simulated and measured characteristics would be in better agreement. In comparison to the circulator, the designed double isolator ensures high isolation, however, the increase of the insertion losses is also observed. The explanation of this effect lies in the fact, that the signal passes twice through the ferrite junction. In the frequency range from 11 to 13.5 GHz the reflection losses are better than 10 dB, insertion losses are about 5 dB and isolation is better than 30 dB.

The obtained high level of isolation encouraged us to develop the double isolator as an integrated planar structure. The even excitation of the FCL sections was realized directly from three-strip line, as in the case of the circulator. Instead of using coaxial loads, as in previous example, the remaining ports of the structure were terminated with the lumped resistors. The utilization of the direct connection between FCL junctions (described in [8, 10]) makes the structure more compact. Fig. 13 shows a photograph of the fabricated structure. The measured characteristics of the double isolator are presented in Fig. 14. The device ensures average reflection losses better than 10 dB in the band from 11 to 14 GHz. In this frequency range the average insertion losses are about 4.5 dB, which is similar to the values presented in [5, 10]. In the investigated frequency range the isolation is better than 16 dB.

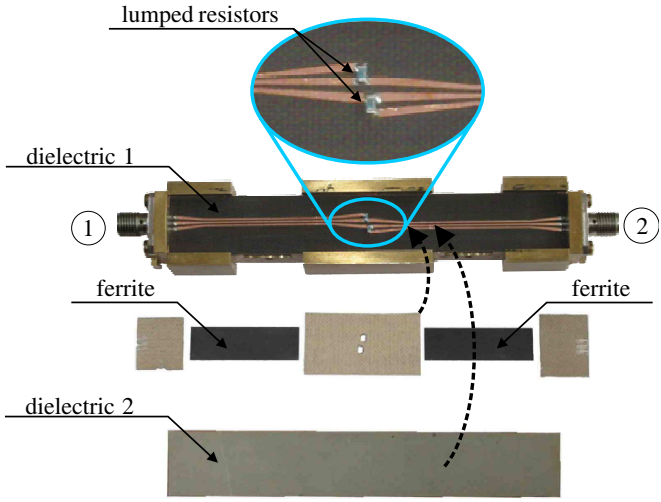

Figure 13. Photograph of the realized planar double isolator containing lumped resistors.

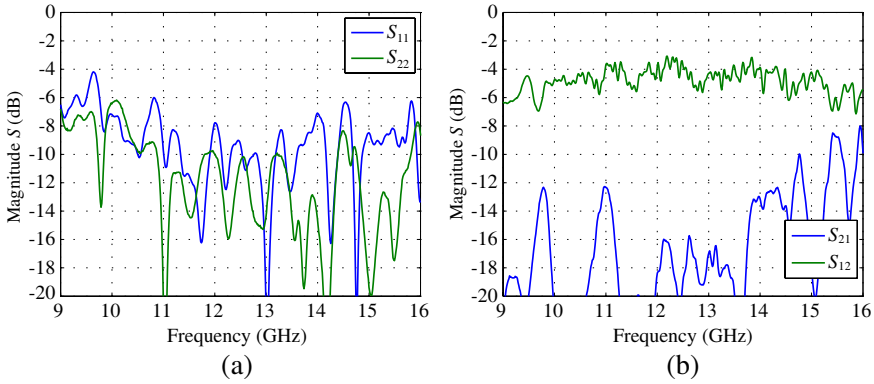

Figure 14. Measured scattering matrix of the planar double isolator: (a) reflection losses, (b) insertion losses and isolations.

It can be seen, that the results obtained for the integrated device are similar to those obtained by cascading measured FCL circulators except of the isolation characteristic. In the integrated structure the isolation deterioration is observed. This is the result of the ports mismatch while using soldered lumped resistors.

5. CONCLUSION

The novel ferrite coupled line junction was proposed for application in nonreciprocal devices. The junction was realized using section of the coplanar three-strip line placed on the longitudinally magnetized dielectric-ferrite substrate. The wave parameters and fields distribution of the fundamental modes in the dielectric and ferrite guide were calculated using SDA. The MM method was utilized to calculate the scattering matrix of the ferrite junction. The obtained results were verified by comparing then with HFSS simulations. The approach allows to obtain the results faster then by using commercial simulators and therefore can be utilized in optimization process to design sections of various nonreciprocal devices. The obtained S-matrix was used to design the circulator and the double isolator. Predicted performance of the designed devices was verified experimentally. Measured average insertion losses of the circulator were about 2.7 dB and isolations were about 12 dB in the frequency range 10–14 GHz. The compact structure of the integrated planar double isolator in the experiment showed average reflection losses better than 10 dB in the frequency range from 11 to 14 GHz. The average insertion losses were about 4.5 dB and isolation better than 16 dB. The obtained insertion losses were comparable with the results found in literature. The nonreciprocal behavior of all designed devices was clearly shown. The further work should be focused on the improvement of the even excitation of FCL junction and the realization of the matching in the integrated double isolator.

ACKNOWLEDGMENT

This work was supported by Polish Ministry of Science and Higher Education from sources for science in the year 2011 under Contract No. 0215/T02/2010/70.

APPENDIX A.

In Chapter 2 the matrices $\mathbf{X}$ take the form

$$\mathbf{X}_1 = \begin{bmatrix} X^{(1,1)}_{+e,+e} & X^{(1,1)}_{+o,+e} & 0 & 0 \\ X^{(1,1)}_{+e,+o} & X^{(1,1)}_{+o,+o} & 0 & 0 \\ X^{(0,1)^*}_{+1,+e} & X^{(0,1)^*}_{+1,+o} & 0 & 0 \\ X^{(0,1)^*}_{+2,+e} & X^{(0,1)^*}_{+2,+o} & 0 & 0 \end{bmatrix}, \quad \mathbf{X}_2 = \begin{bmatrix} X^{(1,1)}_{-e,+e} & X^{(1,1)}_{-o,+e} & 0 & 0 \\ X^{(1,1)}_{-e,+o} & X^{(1,1)}_{-o,+o} & 0 & 0 \\ X^{(0,1)^*}_{+1,-e} & X^{(0,1)^*}_{+1,-o} & 0 & 0 \\ X^{(0,1)^*}_{+2,-e} & X^{(0,1)^*}_{+2,-o} & 0 & 0 \end{bmatrix},$$

$$\mathbf{X}_3 = \begin{bmatrix} X^{(0,1)}_{+1,+e} & X^{(0,1)}_{+2,+e} & X^{(0,1)}_{-1,+e} & X^{(0,1)}_{-2,+e} \\ X^{(0,1)}_{+1,+o} & X^{(0,1)}_{+2,+o} & X^{(0,1)}_{-1,+o} & X^{(0,1)}_{-2,+o} \\ X^{(0,0)^*}_{+1,+1} & X^{(0,0)^*}_{+1,+2} & X^{(0,0)^*}_{+1,-1} & X^{(0,0)^*}_{+1,-2} \\ X^{(0,0)^*}_{+2,+1} & X^{(0,0)^*}_{+2,+2} & X^{(0,0)^*}_{+2,-1} & X^{(0,0)^*}_{+2,-2} \end{bmatrix},$$

$$\mathbf{X}_4 = \begin{bmatrix} 0 & 0 & X^{(2,2)}_{-e,-e} & X^{(2,2)}_{-o,-e} \\ 0 & 0 & X^{(2,2)}_{-e,-o} & X^{(2,2)}_{-o,-o} \\ 0 & 0 & X^{(0,2)^*}_{-1,-e} & X^{(0,2)^*}_{-1,-o} \\ 0 & 0 & X^{(0,2)^*}_{-2,-e} & X^{(0,2)^*}_{-2,-o} \end{bmatrix}, \quad \mathbf{X}_5 = \begin{bmatrix} 0 & 0 & X^{(2,2)}_{+e,-e} & X^{(2,2)}_{+o,-e} \\ 0 & 0 & X^{(2,2)}_{+e,-o} & X^{(2,2)}_{+o,-o} \\ 0 & 0 & X^{(0,2)^*}_{-1,+e} & X^{(0,2)^*}_{-1,+o} \\ 0 & 0 & X^{(0,2)^*}_{-2,+e} & X^{(0,2)^*}_{-2,+o} \end{bmatrix},$$

$$\mathbf{X}_6 = \begin{bmatrix} X^{(0,2)}_{+1,-e} & X^{(0,2)}_{+2,-e} & X^{(0,2)}_{-1,-e} & X^{(0,2)}_{-2,-e} \\ X^{(0,2)}_{+1,-o} & X^{(0,2)}_{+2,-o} & X^{(0,2)}_{-1,-o} & X^{(0,2)}_{-2,-o} \\ X^{(0,0)^*}_{-1,+1} & X^{(0,0)^*}_{-1,+2} & X^{(0,0)^*}_{-1,-1} & X^{(0,0)^*}_{-1,-2} \\ X^{(0,0)^*}_{-2,+1} & X^{(0,0)^*}_{-2,+2} & X^{(0,0)^*}_{-2,-1} & X^{(0,0)^*}_{-2,-2} \end{bmatrix},$$

where elements X of matrices $\mathbf{X}$ are defined as

$$X^{(a,b)}_{s_1 n,\, s_2 m} = \iint\limits_{x,y} \left(E^{(a)}_{x_{s_1 n}} H^{(b)^*}_{y_{s_2 m}} - E^{(a)}_{y_{s_1 n}} H^{(b)^*}_{x_{s_2 m}} \right) \mathrm{d}x\mathrm{d}y \qquad \text{(A1)}$$

where (a) and (b) describe the number of section $(0, 1, 2)$, subscripts n and m define the modes propagated in each section of FCL junction ((e) and (o) are even and odd modes in the dielectric sections, respectively; (1) and (2) are the modes in the ferrite section). The subscripts s_1 and s_2 define the forward $(+)$ and backward $(-)$ direction of the wave propagation.

REFERENCES

1. Mazur, J. and M. Mrozowski, "On the mode coupling in longitudinally magnetized waveguiding structures," *IEEE Transactions on Microwave Theory and Techniques*, Vol. 37, No. 1, 159–164, January 1989.
2. Cao, M., R. Pietig, H. C. Wu, and R. G. Gossink, "Perturbation theory approach to the ferrite coupled stripline," *2004 IEEE MTT-S International Microwave Symposium Digest*, Vol. 3, 1903–1906, May 2004.

3. Queck, C. K. and L. E. Davis, "Microstrip and stripline ferrite-coupled-lines (FCL) circulators," *IEEE Transactions on Microwave Theory and Techniques*, Vol. 50, No. 12, 291–2917, December 2002.
4. Queck, C. K. and L. E. Davis, "Novel folding technique for planar ferrite-coupled-line circulators," *IEEE Transactions on Microwave Theory and Techniques*, Vol. 52, No. 5, 1369–1374, May 2004.
5. Queck, C. K. and L. E. Davis, "Broad-band three-port and four-port stripline ferrite coupled line circulators," *IEEE Transactions on Microwave Theory and Techniques*, Vol. 52, No. 2, 625–632, February 2004.
6. Mazur, J., M. Solecka, R. Poltorak, and M. Mazur, "Theoretical and experimental treatment of a microstrip coupled ferrite line circulator," *IEE Proceedings — Microwaves, Antennas and Propagation*, Vol. 151, No. 6, 477–480, December 2004.
7. Cao, M. and R. Pietig, "Ferrite coupled-line circulator with reduced length," *IEEE Transactions on Microwave Theory and Techniques*, Vol. 53, No. 8, 2572–2579, August 2005.
8. Marynowski, W., A. Kusiek, and J. Mazur, "Microstrip ferrite coupled line isolators," *XVI International Microwaves, Radar and Wireless Communications Conference*, Vol. 1, 342–345, Krakow, Poland, May 2006.
9. Yang, L.-Y. and K. Xie, "Design and measurement of nonuniform ferrite coupled line circulator," *Journal of Electromagnetic Waves and Applications*, Vol. 25, No. 1, 131–145, 2011.
10. Marynowski, W., A. Kusiek, and J. Mazur, "Microstrip four-port circulator using a ferrite coupled line section," *AEU — International Journal of Electronics and Communications*, Vol. 63, No. 9, 801–808, July 2008.
11. Marynowski, W. and J. Mazur, "Treatment of the three strip coplanar lines on the ferrite," *XVII International Microwaves, Radar and Wireless Communications Conference*, Vol. 1, 135–138, Wroclaw, Poland, May 2008.
12. Michalski, J., M. Mazur, and J. Mazur, "Scattering in a section of ferrite coupled microstrip lines: Theory and application in nonreciprocal devices," *IEE Proceedings — Microwaves, Antennas and Propagation*, Vol. 149, Nos. 5–6, 286–290, October–December 2002.
13. Razavipour, H., R. Safian, G. Askari, F. Fesharaki, and H. Mirmohammad Sadeghi, "A new dual-band high power ferrite circulator," *Progress In Electromagnetics Research C*, Vol. 10, 15–24, 2009.

14. Sajin, G., S. Simion, F. Craciunoiu, A. A. Muller, and A. C. Bunea, "CRLH CPW antenna on magnetically biased ferrite substrate," *Journal of Electromagnetic Waves and Applications*, Vol. 24, Nos. 5–6, 803–814, 2010.
15. Zahwe, O., B. Sauviac, B. Abdel Samad, J. P. Chatelon, and J. J. Rousseau, "Numerical study of a circulator using YIG thin film with a coplanar structure," *Progress In Electromagnetics Research C*, Vol. 6, 193–207, 2009.
16. Zahwe, O., B. Abdel Samad, B. Sauviac, J. P. Chatelon, M. F. Blanc Mignon, J. J. Rousseau, M. Le Berre, and D. Givord, "YIG thin film used to miniaturize a coplanar junction circulator," *Journal of Electromagnetic Waves and Applications*, Vol. 24, No. 1, 25–32, 2010.
17. Kusiek, A., W. Marynowski, and J. Mazur, "Investigations of the circulation effects in the structure using ferrite coupled slot-line section," *Microwave and Optical Technology Letters*, Vol. 49, No. 3, 692–696, January 2007.
18. Abdalla, M. A. and Z. Hu, "Multi-band functional tunable LH impedance transformer," *Journal of Electromagnetic Waves and Applications*, Vol. 23, No. 1, 39–47, 2009.
19. Bahri, R., A. Abdipour, and G. Moradi, "Analysis and design of new active quasi circulator and circulators," *Progress In Electromagnetics Research*, Vol. 96, 377–395, 2009.
20. Marynowski, W. and J. Mazur, "Three-strip ferrite circulator design based on coupled mode method," *2009 International Symposium on Antennas and Propagation (ISAP 2009)*, 205–208, Bangkok, Thailand, October 2009.
21. Marynowski, W. and J. Mazur, "Investigations of the double isolator using three-strip ferrite coupled line," *15th Conference on Microwave Techniques, COMITE 2010*, Brno, Czech Republic, April 2010.